*ENGINEERING TRANSACTIONS* • *Engng. Trans.* • **64**, 4, 605–611, 2016
Polish Academy of Sciences • Institute of Fundamental Technological Research (IPPT PAN)
National Engineering School of Metz (ENIM) • Poznan University of Technology

# A New Model of Bone Remodelling

Justyna MIODOWSKA, Jan BIELSKI, Magdalena KROMKA-SZYDEK

*Cracow University of Technology*
*Institute of Applied Mechanics*
Jana Pawła II 37, 31-864 Kraków, Poland
e-mail: justyna.miodowska@pk.edu.pl

The objective of this paper is to propose a mathematical model of bone remodelling, including underload and overload resorption, equilibrium and bone grow states which can occur during healing process. A continuous function of bone density rate vs. mechanical stimulus is proposed. The created model is used to predict the stress-stimulated change in callus density. It is an extension of mathematical descriptions available in literature.

**Key words:** bone remodelling, mandible, callus, mechanical stimulus.

## 1. Introduction

Bone tissue is capable to remodel in response to mechanical internal and external conditions. Bone's mass and geometry can adapt to mechanical stimulus (stress or strain induced) which process is known as functional adaptation. According to the Wolff law [1], a bone has the ability to change its material properties (density) and external architecture to adapt to applied loads via a biological process called remodelling. During this process, both bone resorption and apposition may occur. A bone tissue resorbs when the mechanical stimulus drops below a lower threshold value whereas bone apposition occurs when the load exceeds an upper threshold value. If the mechanical stimulus remains between the threshold values (lazy zone), remodelling does not occur [2]. Moreover, when the mechanical stimulus increases excessively, overload resorption may occur causing bone loss. The current mathematical models of the bone remodelling are often used to model changes in bone density around implants, dental the most [3–6]. Among them a few consider bone resorption due to overload. Moreover there are no such studies in relation to the callus, which is also a bone tissue. The most commonly used approach takes into account three stages: underload resorption, equilibrium, and bone growth (apposition). Lin [6] proposes mathematical description of overload resorption but it results in not physically justified function's discontinuity. This approach is adopted by other authors [7, 8]. Li [9] proposes quadratic equation for continuous description of bone remodelling, but entirely omits the lazy zone (equilibrium state).

## 2. Model and methods

According to the bone remodelling theory the bone tissue can adapt its properties according to different kinds of mechanical stimulus. In this paper, similar to the Weinans theory [10], parameter $\psi$ is chosen as a remodelling stimulus which denotes strain energy density $U$ [J/cm$^2$] per bone mass density $\rho$ [g/cm$^3$] (Fig. 1). It is a local value determined at a material point, very convenient to use because of its scalar character.

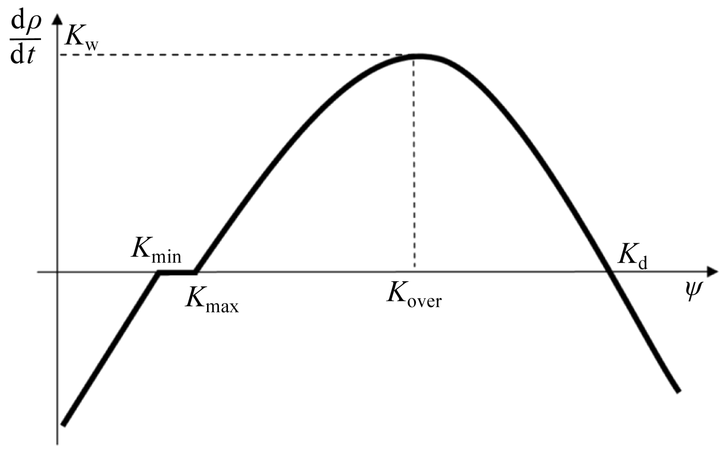


Fig. 1. Bone density rate in relation to mechanical stimulus $\psi$.

The local bone density changes as a function of the mechanical stimulus, following the remodelling rate equation:

$$\frac{d\rho}{dt} = \begin{cases} B(\psi - K_{\min}), & \psi < K_{\min}, \\ 0, & K_{\min} \leqslant \psi \leqslant K_{\max}, \\ D(\psi - K_{\text{over}})^2 + K_{\text{w}}, & \psi > K_{\max}, \end{cases} \tag{2.1}$$

where $B$ and $D$ are remodelling constants, $K_{\min}$, $K_{\max}$, $K_{\text{over}}$ and $K_{\text{d}}$ are the stimulus threshold values. It is noted that there are different relations between density and bone Young's modulus $E$ available. In this paper, following equation is adopted:

$$E = c\rho^3, \tag{2.2}$$

where $c$ is a constant. The ordinary differential equation (2.1) is integrated numerically by using the forward-Euler method:

$$\rho(t + \Delta t) = \rho(t) + \left.\frac{\mathrm{d}\rho}{\mathrm{d}t}\right|_t \cdot \Delta t. \tag{2.3}$$

Using equation (2.3) the change in bone density at each time step is calculated. Then the corresponding elastic modulus is updated according to (2.2). The next step of calculation is then performed using modified material properties. The iterative process continues until a 200 MPa Young's modulus is achieved. According to KNETS [11] such a value indicates a bone union.

## 3. Results

Rectangular cross-section ($b \times h$) is chosen for studying the model's properties. Here, the analysis is mainly addressed to the interval $K_{\max} \leqslant \psi \leqslant K_{\mathrm{d}}$, what means a bone growth. In the first case the study is carried out by applying a tensile force $N$. This results in a homogenous state of stress and strain (a point level analysis). To obtain analytical solution the relations for stress $\left(\sigma = \frac{N}{bh}\right)$, strain $\left(\varepsilon = \frac{\sigma}{E}\right)$ and strain energy density $\left(U = \frac{1}{2E}\sigma^2\right)$ are used. Then the mechanical stimulus can be described as:

$$\psi = \frac{U}{\rho} = E^{-4/3}\frac{N^2}{(bh)^2}. \tag{3.1}$$

It turns out that for a constant in time load value it is impossible to obtain sufficiently high Young's modulus (200 MPa) even after infinitely long time (Fig. 2, solid line). This is due to asymptotic character of the solution of (2.1) for $\psi > K_{\max}$. Namely, initial increase of the density increases the value of denominator in (3.1), whereas nominator remains constant for the unchanged load. Hence, the values of the stimulator tends to $K_{\max}$, what denotes approaching the lazy zone. In order to get the maximum rate of increase in the density the force value should change so as to satisfy:

$$\psi = \frac{\sqrt[3]{c}}{2}E^{-4/3}\frac{N^2}{(bh)^2} = K_{\mathrm{over}}, \tag{3.2}$$

which is equivalent to initially the highest value of the bone remodelling rate $K_{\mathrm{w}}$

$$\frac{\mathrm{d}\rho}{\mathrm{d}t} = K_{\mathrm{w}}. \tag{3.3}$$

This approach, in which the force increases in time, allows to obtain sufficiently high Young's modulus (Fig. 2, dashed line).

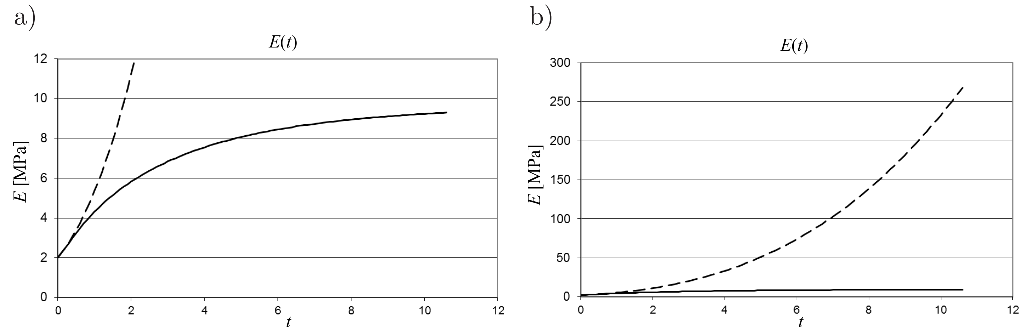


FIG. 2. The Young's modulus in time: asymptotically limited (a) and monotonically increasing (b).

In the second case, the analysis is carried out for a section loaded with constant values of bending moment $M$ and shear force $T$. This initiates heterogonous state of stress which results in unavoidable material inhomogeneity. A complex stress state implies that the value of strain energy density varies along the height of the section $-h/2 \leqslant z \leqslant h/2$. Strain energy density:

$$U(z) = \frac{1}{2E(z)}[\sigma(z)]^2 + \frac{1+\nu}{E(z)}[\tau(z)]^2. \tag{3.4}$$

For variable elastic modulus stress distribution is not elementary. Normal stress:

$$\sigma = \frac{M \cdot E(z) \cdot (z - z_0)}{I_E}, \qquad I_E = b \int_{-h/2}^{h/2} E(z) \cdot (z - z_0) \cdot z \, \mathrm{d}z, \tag{3.5}$$

where $I_E$ [$\mathrm{mm}^4 \cdot \mathrm{MPa}$] denotes the generalized moment of inertia. Shear stress:

$$\tau = \frac{T \cdot S_E(z)}{I_E \cdot b}, \qquad S_E(z) = b \int_{-h/2}^{z} E(\xi) \cdot (\xi - z_0) \, \mathrm{d}\xi, \tag{3.6}$$

where $S_E$ [$\mathrm{mm}^3 \cdot \mathrm{MPa}$] denotes the generalized static moment about neutral axis of section cut-off lying one side of level $z$ and $z_0$ stands for a possible relocation of a section neutral axis ($z_0 = 0$ for symmetrical case with $N = 0$). Several variants are presented (Fig. 3) for constant in time $M$ and $T$. Unfortunately, the results of integration do not lead to satisfactory density distribution in the

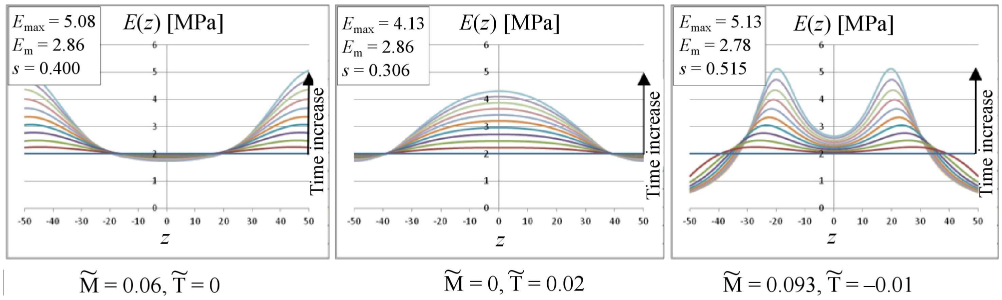


Fig. 3. The Young modulus $z$-distribution for constant values of shear force and bending moment.

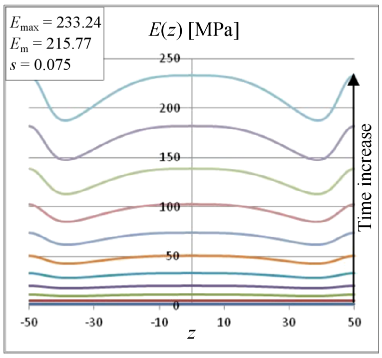


Fig. 4. The Young's modulus $z$-distribution improved by the control algorithm.

entire analyzed section, neither with the value, nor homogeneity. Homogeneity is evaluated using three parameters: maximal ($E_{\max}$) and mean ($E_{\mathrm{m}}$) Young's modulus together with standard deviation:

$$s = \sqrt{\frac{\int\limits_{-h/2}^{h/2} \left(\frac{E(z)}{E_{\mathrm{m}}} - 1\right)^2 \mathrm{d}z}{h}}.$$

The less is $s$ and the less is difference $E_{\max} - E_{\mathrm{m}}$ the better (the more homogenous) is the obtained distribution of $E(z)$. As expected, similarly to homogenous stress state, it is still impossible to obtain sufficiently high value of Young's modulus keeping constant in time load parameters $M$ and $T$. Moreover, the unwanted resorption is met instead of the growth at some regions.

Taking conclusion from the constant-load analysis, a control algorithm is proposed to improve homogeneity of the elasticity modulus. We require that at selected points of $z$ axis (0 and $h/2$) the stimulus value $\psi$ is kept constant in time and equals $K_{\text{over}}$. It ensures maximum increase of the density at the outer and the middle fibers of cross-section. Using (2.2), (3.4), (3.5), (3.6) we get:

$$\psi(z) = \frac{U}{\rho}(z) = \frac{\sqrt[3]{c}}{2} \cdot \frac{M^2(z-z_0)^2 \cdot [E(z)]^{2/3}}{I_E^2} + \frac{\sqrt[3]{c}(1+\nu)}{[E(z)]^{4/3}} \cdot \frac{T^2\,[S_E(z)]^2}{I_E^2 \cdot b^2}. \tag{3.7}$$

Satisfying $\psi(0) = \psi(h/2) = K_{\text{over}}$, and due to section's symmetry and lack of axial force $N$ (which denotes $z_0 = 0$ and $S_E(h/2) = 0$), we come to a set of equations to determine values of the shear force and the bending moment:

$$\frac{\sqrt[3]{c}(1+\nu)}{[E(0)]^{4/3}} \cdot \frac{[S_E(0)]^2}{I_E^2 \cdot b^2} \cdot T^2 = K_{\text{over}}, \tag{3.8}$$

$$\frac{\sqrt[3]{c}}{2} \cdot \frac{\dfrac{h^2}{4} \cdot \left[E\left(\dfrac{h}{2}\right)\right]^{2/3}}{I_E^2} \cdot M^2 = K_{\text{over}}. \tag{3.9}$$

Since the distribution of $E(z)$ evolves in time according to (2.1) and (2.2), so do $S_E$ and $I_E$ ((3.5), (3.6)). Hence, equations (3.6) and (3.9) define $T$ and $M$ as functions of time.

## 4. Conclusion

The proposed new model provides a continuous function which describes the callus remodelling process. The analyses indicate that obtaining a sufficiently high value of callus modulus is possible only using the time-varying load parameters since constant loads lead to asymptotic limitation of the Young modulus value usually much below the required level. Moreover, for a complex stress state, undesirable distribution is observed. It is also proved that a quasi-optimal time programs are possible, which lead to more homogenous distribution with required value of the modulus. The investigated bone remodelling model is suitable for more complex finite element calculations with true bone geometry.

## References

1. Wolff J., *The law of bone remodeling*, Springer-Verlag, Berlin 1986.

2. Mellal A., Wiskott H.W.A, Botsis J., Scherrer S.S., Belser U.C., *Stimulating effect of implant loading on surrounding bone. Comparison of three numerical models and validation by in vivo data*, Clinical Oral Implant Research, **15**(2): 239–248, 2004, doi: 10.1111/j.1600-0501.2004.01000.x.

3. Chou H-Y., Jagodnik J.J., Muftu S., *Predictions of bone remodeling around dental implant system*, Journal of Biomechanics, **41**(6): 1365–1373, 2008, doi: 10.1016/j.jbiomech.2008.01.032.

4. Field C., Li Q., Li W., Thompson M., Swain M., *A comparative mechanical and bone remodelling study of all-ceramic posterior inlay and onlay fixed partial dentures*, Journal of Dentistry, **40(1)**: 48–56, 2012, doi: 10.1016/j.jdent.2011.10.003.

5. Lian Z.Q., Guan H., Loo Y.C., *Optimum degree of bone-implant contact in bone remodelling induced by dental implant*, Procedia Engineering, **14**: 1972–2979, 2011, doi: 10.1016/j.proeng.2011.07.374.

6. Lin C-L., Lin Y-H., Chang S-H., *Multi-factorial analysis of variables influencing the bone loss of an implant placed in the maxilla: Prediction using FEA and SED bone remodeling algorithm*, Journal of Biomechanics, **43**(4): 644–651, 2010, doi: 10.1016/j.jbiomech.2009.10.030.

7. Wang C., Fu G., Deng F., *Difference of natural teeth and implant-supported restoration: a comparison of bone remodeling simulations*, Journal of Dental Science, **10(2)**: 190–200, 2015, doi: 10.1016/j.jds.2014.11.001.

8. Wang C., Li Q., McClean C., Fan Y., *Numerical simulation of dental bone remodeling induced by implant-supported fixed partial denture with or without cantilever extension*, International Journal for Numerical Methods in Biomedical Engineering, **29**(10): 1134–1147, 2013, doi: 10.1002/cnm.2579.

9. Li J. *et al.*, *A mathematical model for simulating the bone remodeling process under mechanical stimulus*, Dental Materials, **23**(9): 1073–1078, 2007, doi: 10.1016/j.dental.2006.10.004.

10. Weinans H., Huiskes R., Grootenboer H.J., *The behavior of adaptive bone-remodeling simulation models*, Journal of Biomechanics, **25(12)**: 1425–1441, 1992, doi: 0.1016/0021-9290(92)90056-7.

11. Knets I., Vitins V., Cimdins R., Laizans J., *Biomechanical behaviour of system bone-callus-implant*, Proceedings of 10th Conference of the European Society of Biomechanics, J. Vander Sloten et al. [Ed.], Leuven, p. 97, August 28–31, 1996.

*Received October 11, 2016; accepted version November 23, 2016.*